NB_3SN AND NBTI FOR HIGH FIELD APPLICATIONS WITH EMPHASIS TO FUSION MAGNETS

J.L. Duchateau
Association EURATOM-CEA, CEA/DSM/DRFC CEA-Cadarache
F-13108 Saint Paul Lez Durance Cedex France

Abstract
This paper gives a view of the present situation of the two main materials used for high field superconducting magnets, namely Nb_3Sn and NbTi. Two specific issues are discussed in detail, the strain sensitivity of large Nb_3Sn cables and the potential for a further increase of the maximum field in accelerator magnets through Ta addition in NbTi.

1. INTRODUCTION

Superconducting conductors have to face the request of increasing field for magnets. Several kinds of answers can be brought to this request depending on the application. This trend is illustrated in fusion with the development of Nb_3Sn Cable in Conduit Conductors and the degradation effect linked to bending strain. In Particle Physics there is the idea that Tantalum addition in NbTi could avoid the mutation to the more expensive Nb_3Sn. This idea is examined taking into account in a realistic way the design margins.

2. CABLES IN CONDUIT CONDUCTORS FOR FUSION APPLICATION

In the framework of ITER programs, the ITER partners have carried out an extensive research and development programme for the last 10 years. This program aimed at designing and industrialising the high current (40-70 kA), high field conductors adapted to the superconducting magnet systems of this machine [1]. Europe has been involved in this programme.

The solution retained for the ITER conductor, is the so-called Cabled in Conduit Conductor (CICC), the original concept of which was developed by Hoenig in 1974 [2]. Substantial progress has been made to adapt this concept to the requirements of fusion technology. One major step was the

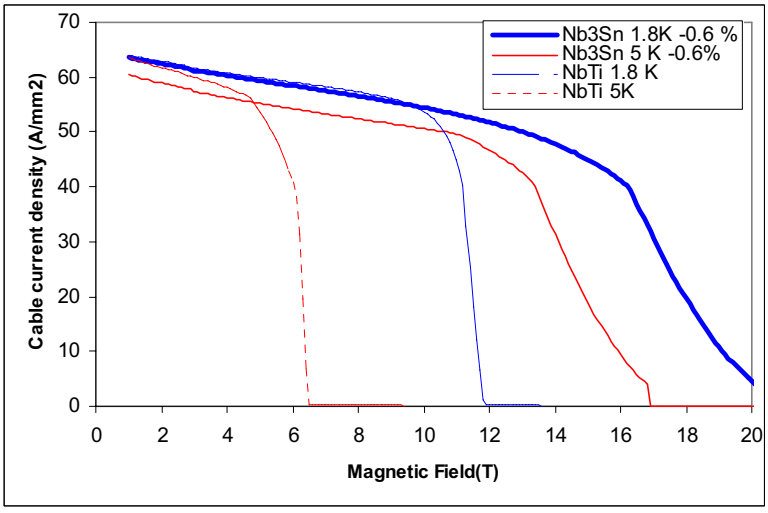

Figure 1: Range of application of NbTi and Nb_3Sn as a function of field and temperature for a typical Cable in Conduit for fusion (15 s fast discharge)

introduction of Nb_3Sn, a more performing superconducting material required by the high level of magnetic field in ITER (12-13 T).

The range of application of NbTi or Nb_3Sn as a function of field and temperature is presented in Figure 1 with the associated current density which is relatively low in comparison with the design current densities in magnets for particle accelerators, and includes the helium with a typical void fraction of 35 %.

In the framework of this program, two model coils were manufactured and tested: the Central Solenoid Model Coil (CSMC) [3, 4, 5, 6] and the Toroidal Field Model Coil (TFMC) [7, 8, 9]. The TFMC program was mainly taken in charge by Europe. Nine hundred meters of TFMC conductor in five pieces were successfully provided for the manufacture of these model coils.

3. AN APPLICATION OF CICC: THE ITER TF MODEL COIL AND ITS CONDUCTOR

3.1 The coil

The winding pack of the TFMC is made by stacking 5 double pancakes (DP1, DP2, DP3, DP4, DP5) with a racetrack shape (Figure 2). Each double pancake is embedded in the spiral grooves machined on both sides of stainless steel plates. The total length of conductor is around 800 meters. The winding pack is enclosed in an 80 mm thick walled stainless steel case.

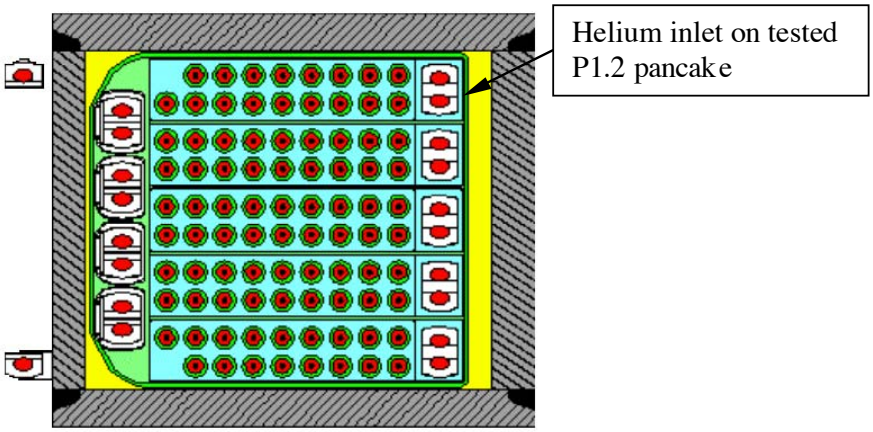

Figure 2: TFMC cross section showing the system of 5 double pancakes embedded in plates and surrounded by a casing.

3.2 The conductor

The cable (see Figure 3) is made of six petals cabled around a central metallic spiral of 10 mm internal diameter and 1 mm thick. The characteristics of the cable are presented in Table 1.

Figure 3: TFMC conductor (Φ=40.7 mm)

Table 1: TFMC conductor characteristics

Cable pattern	3x3x5x4x6
Corresponding twist pitches	25mm/62mm/109 mm/168 mm/425 mm
Number of superconducting strands	720
Number of copper strands	360
Local void fraction in the annulus	36 %
Central hole inner diameter	10 mm
Cable space diameter	37.5 mm
Jacket thickness	1.6 mm

3.3 The strand

Four tons of strands have been produced by Europa Metalli (EM) in Italy. A cross section of the strand is reported in Fig. 4.

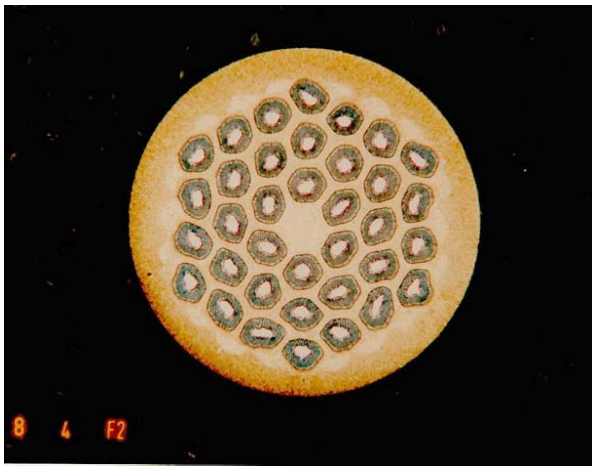

Figure 4: EM-LMI Nb_3Sn strand for TFMC (Φ=0.81 mm)

3.4 Exploration of the limits of the conductor [10]

After current ramping and plateau, the helium entering P1.2 pancake (at the inner joint) was slowly heated. The temperature was simultaneously increased in neighbouring P1.1 pancake to limit the heat exchange between the two pancakes. The voltage drop over the whole pancake was measured using co-wound voltage taps as visible in Figure 5.

The temperature presented in the Figure 5 is the inlet temperature before the inner joint and there is no additional temperature sensor along the conductor. It is known however that the most critical point, where the field is maximum, is situated at about 2 meters from the joint area.

As visible in Figure 5, the voltage increased according to the inlet temperature illustrating the so-called current sharing regime. The conductor is so stable that it is possible to recover after a temperature excursion of 0.5 K above the current sharing temperature.

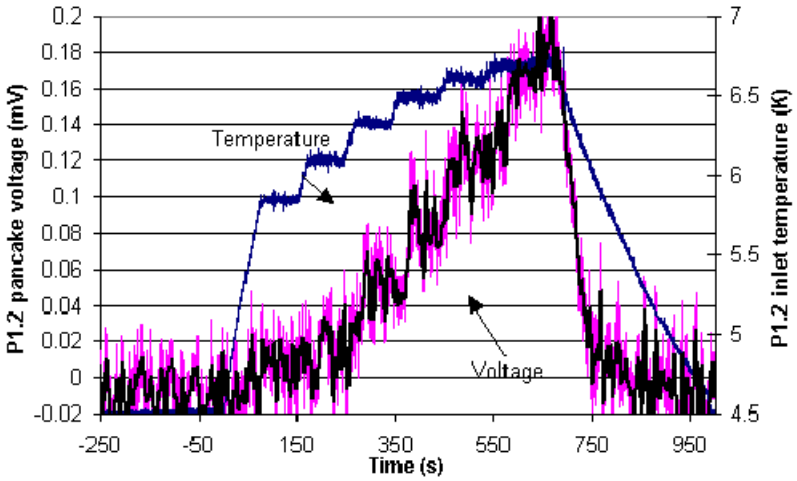

Figure 5: Exploration of the TFMC limits by increasing the P1.2 temperature inlet. Current sharing temperature is reached in the second temperature plateau(Test: 21 November 2002)

4. SENSITIVITY OF NB3SN TO COMPRESSION IN STAINLESS STEEL JACKETED CICC

The sensitivity of Nb3Sn to compressive strain is well known. According to theory the effective strain ($\varepsilon_{effective}$) in a stainless steel conductor is the sum of two terms, namely the thermal compression ε_o due to thermal heat treatment, and the elongation ε_{op} which appears due to the electromagnetic forces in operation.The total strain can be written as follows:

$$\varepsilon_{effective} = \varepsilon_o + \varepsilon_{op} \quad (1)$$

According to theory the maximum value (in absolute) which can be awaited for ε_o is the differential thermal contraction from 923 K to 4 K between steel and Nb3Sn. This parameter is not

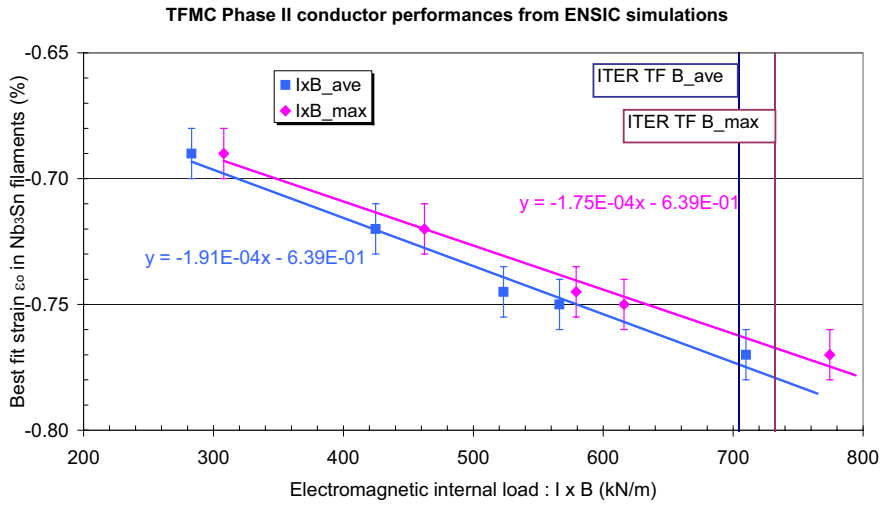

Figure 6. Influence of internal load on ε_0 in TFMC experiment

well characterized, moreover the cable void fraction can attenuate this effect due to imperfect bonding but this phenomenon is not well characterized either. The exploration of the conductor limits, knowing all the others parameters of the Summers model, showed that ε_o is depending on the transverse magnetic load in a way which is not completely understood. This is one of the main results obtained in the TFMC experiment concerning the filament strain $\varepsilon_o$and is reported in Fig. 6. From the TFMC experiment, the following points were highlighted:

1. The Nb3Sn filament strain ε_o is depending on the magnetic load which was not expected by a simple classical model
2. In phase II experiment the TFMC was tested in a magnetic load range relevant to ITER.
3. At ITER TF relevant magnetic load the filament compression ε_o is larger than expected: [0.75, 0.79] instead of 0.6 in ITER design
4. The 'n' value (around 10) is lower than expected (20)

Points 2 through 4 suggest that the simple model of compression during cool down from reaction and stretching during operation is too simple and not effective to account for the experiment. Bending strain, whose effects were initially described by Ekin [11] in 1980 could be an explanation. In the case of CICC's, however, bending strain is not originated as envisaged by Ekin by reacting Nb3Sn strands and winding them on a mandrel. Indeed, according to the model developed by Mitchell [12], the bending strain in a CICC could be induced by the twist of the strands inside the jacket and can appear during thermal compression induced by the cool down from reaction temperature before any loading, or during coil energization due to magnetic load. In this model the strain can vary across the filament section and along the strand with a wavelength of typically 5 to 10 mm. A finite element model has been developed by Mitchell but no quantitative dependency can be given. The following parameters are supposed to play a role :

- the twist pitch of the strand can affect the current redistribution between filaments within a strand and average the effect of strain distribution across the strand section;
- the geometry of the strand and associated effective resistivity of the matrix can also help to average the strain. This can be very different from one company to another;
- the cable void fraction can also play a role to minimize this effect.

4.1 Open issues on strain sensitivity in Nb_3Sn

Based on the discussion above, we can summarise the open issues on strain sensitivity in Nb3Sn in the following list:

- Is the differential thermal contraction applied in the same way in a Cable in Conduit and in a wire soldered on a spring (tests made at Durham and Twente on Walters type spring) ?
- Is applying an axial stress on the wire to strongly compress it, an exact simulation of the effect of the thermal contraction in a CICC ?
- Is the Summers model correctly accounting for behaviour of strands under high compressive strain which are related to stainless steel jackets ? Experiments at Durham and at Twente showed that the decrease in J_{noncu} is more pronounced at high compressions.
- Mechanical properties of Nb3Sn are different according to the vendors : what is the simpler short sample representative of the mechanical properties of the material embedded in a conduit ?

4.2 Experiments to improve understanding of bending strain in representative stainless steel jacketed subsize samples

Experiments have already been performed in the past to improve the understanding of Nb_3Sn under compression on subsize samples (see, as an example, the small cable cross section in Figure 7 and the

corresponding pulling experiment results reported in Figure 8)[13]. These samples did not exhibit a behaviour very different from what was expected from the Summers law.

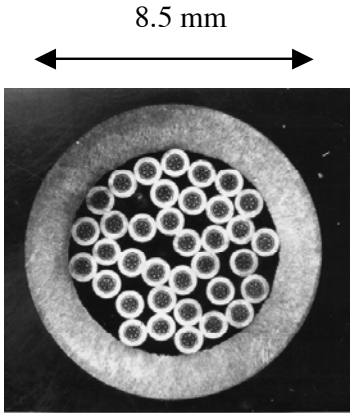

Figure 7: Subsize stainless steel jacketed cable in conduit

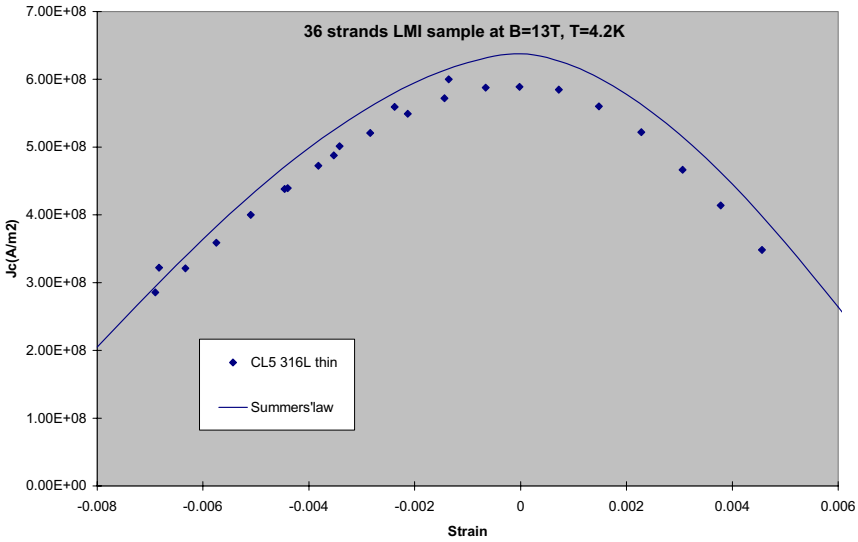

Figure 8: Stretching a subsize (36 strands) Nb_3Sn conductor in the FBI facility

EM strand 12 T 4.2 K (A316 jacket) 1997

A new program has recently been launched in Europe with advanced strands for ITER, to explore the influence of various parameters on bending strain (twist pitch, void fraction, type of strands). The experimental test will be carried out at the FBI test facility at FZK with an improved sensitivity in voltage measurement to gain information about the n value.

Even simpler samples made of one strand such as the one presented in Figure 9, which consists of a single strand jacketed in a stainless steel pipe, can help to explore strain and investigate compression effect on Ic.

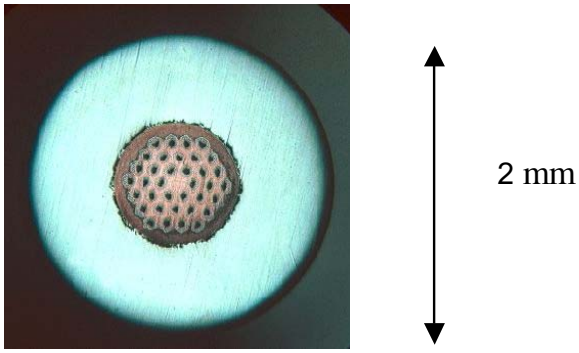

Figure 9: strand manufactured at ENEA to be stretched at FZK on FBI test facility to investigate compression and effect on Ic (courtesy of ENEA)

5. PUSHING NBTI AT ITS LIMITS IN PARTICLE PHYSICS, CAN TANTALUM ADDITION HELP ?

As illustrated in Figure 1, NbTi conductor can perfectly operate at 11 T, at low current density. In practice this possibility was not used extensively. Only the operation of the Large Coil Task coil demonstrated this capacity [14] and this coil was besides used in subcooled mode to provide a background field for the TFMC. A general question is whether tantalum addition can help in Particle Physics to increase the field of dipoles and offer a cheaper solution than the use of Nb_3Sn. This point will be illustrated based on the practical example on LHC dipoles.

5.1 Operation point of LHC dipoles

At 1.9 T and 8.33 T the LHC dipole conductor is far from the critical properties of the conductor. Typically at 8.33 T and 11850 A at constant field, the margin in temperature is 2 K and the margin in critical current is 50 %. This can be presented analytically as well as graphically.

The current density in NbTi at 8.33 T and 11850 A in the cable (nominal conditions) is J=1259 A/mm2. The critical current density in these conditions is:

$$J_c(1.9\ K, 8.33\ T) = 2482\ A/mm^2$$

A simple description of critical current density as a function of field and temperature can be given due to the linear behaviour of the critical current density as a function of field, the parameters of the model are probably not completely exact but the method remains valid:

$$J_c(T,B) = -a[B+B_{c20}((T/T_{c0})^{1.7}-1)] \qquad B_{c20} = 13.87\ T \qquad T_{c0} = 9.2\ K \qquad a = 625$$

The current sharing temperature Tcs of the LHC dipole at this current density is by definition:

$$J = -a[B+B_{c20}((T_{cs}/T_{c0})^{1.7}-1)]$$

$$T_{cs} = T_{c0}[1-J/(a\,B_{c20})-(B/B_{c20})]^{1/1.7} = 4.12\ K$$

These margins can also be illustrated graphically in Figure 10.

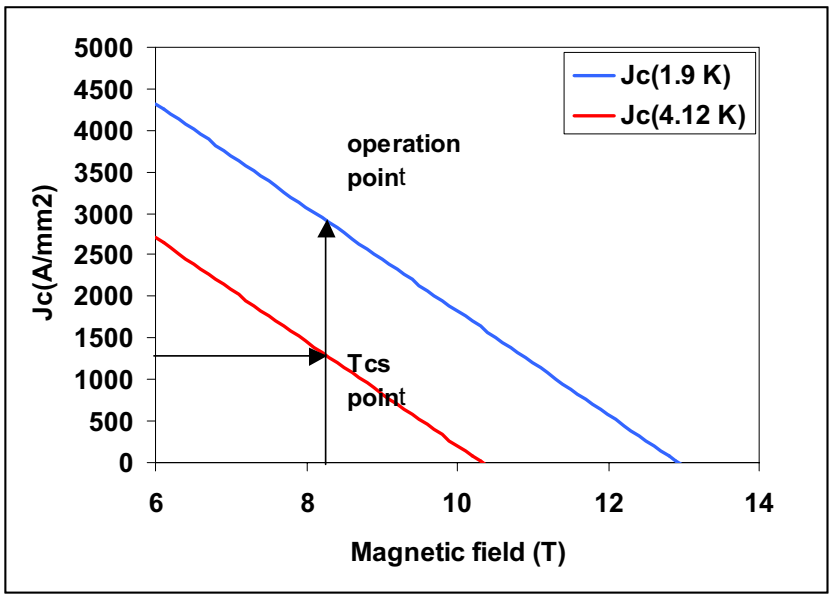

Figure 10 : Tcs in LHC as compared with the (1.9K and 8.33 T) point.

5.2 Consequences of tantalum addition.

From the preceding section it can be seen that the design temperature point of the dipole is not 1.9 K but rather 1.9 K $+\Delta T_{op} + \Delta T_{margin}$, where ΔT_{op} is the temperature increase in operation due to the beam heating, and ΔT_{margin} is the temperature margin to ensure current stability. The sum of these two terms for a LHC dipole, is large due to magnetic instabilities probably associated with the very high mechanical forces.

It is well known that the help of tantalum, whatever the tantalum content in titanium, is effective only if the field is higher that 11 T, in addition the increase in current density vanishes if the design temperature is higher than 1.8 K. It is the case for LHC dipoles at least due to beam heating but also due to additional temperature margin.

6. CONCLUSION

The use of tantalum in LHC dipoles could be envisaged only for a field higher than 11 T. Even in this range of field, the use is questionable due to the design temperature which is substantially higher than 1.8 K.

7. REFERENCES

[1] Duchateau J L, Spadoni M, Salpietro E, Ciazynski D, Ricci M, Libeyre P, della Corte A 2002 Supercon. Sci. Techno. 15 817-829

[2] Hoenig M O et al. 1975 Proc. 5 th Int. Conf. Mag. Tech. (Roma Italy Laboratori Nazionale del CNEN) 519 524

[3] Jayakumar R et al. 1998 Proc. 15 th Int. Conf. Mag. Tech. (Beijing: Science Press) 357 360

[4] Nakajima H et al. 1998 Proc. 15 th Int. Conf. Mag. Tech. (Beijing: Science Press) 361 364

[5] Martovetsky N et al. 2001 IEEE Trans. Appl. Supercon. **11** 2030 2033

[6] Ando T et al. 2002 IEEE Trans. Appl. Supercon. 12 496 499

[7] Salpietro E 2002 IEEE Trans. Appl. Supercon. 12 623 626

[8] Ulbricht A and the ITER L2 project Team 2003 Proc. of the 22 nd SOFT To be published.

[9] Nicollet S et al 2003 Proc. of the 19 th Int. Cryo. Eng. Conf. 161 164

[10] Duchateau J.L et al. 2004 Supercon. Sci. Techno. 17 241-249

[11] Ekin J W 1980 “Filamentary A15 superconductors” editors M. Suenaga and A.F Clark Plenum Press

[12] Mitchell N 2003 Cryogenics 43 255-270.

[13] Specking W, Duchateau J L, Decool P 1998 Proc. 15 th Int Conf. On Magnet Tech. (Beijing: Science Press) 1210 1213

[14] Heller R et al. 1998 Cryogenics 38 519